Investigation of 1,3,5-Triaza-7-phosphaadamantane-Stabilized Silver Nanoparticles as Catalysts for the Hydration of Benzonitriles and Acetone Cyanohydrin

Tobias J. Sherbow,[†] Emma L. Downs,[†] Richard I. Sayler,[†] Joshua J. Razink,[‡] J. Jerrick Juliette,[§] and David R. Tyler*[,†]

[†]Department of Chemistry, University of Oregon, Eugene, Oregon 97403, United States
[‡]Center for Advanced Materials Characterization in Oregon, University of Oregon, Eugene, Oregon 97403, United States
[§]Shell Oil Products LLC, Shell Deer Park Site, Deer Park, Texas 77536, United States

S *Supporting Information*

ABSTRACT: A straightforward synthesis of water-soluble silver nanoparticles stabilized by PTA (1,3,5-triaza-7-phosphaadamantane, a water-soluble phosphine ligand) ligands was developed. The nanoparticles were thoroughly characterized by ultraviolet–visible spectroscopy, ^{31}P nuclear magnetic resonance spectroscopy, transmission electron microscopy, and energy dispersive X-ray spectroscopy. The effectiveness of the Ag–PTA nanoparticles as catalysts for the hydration of nitriles to amides in water under mild conditions was explored using a series of substituted benzonitriles and cyanohydrins. In comparison to all previously investigated homogeneous catalysts, the Ag–PTA system excels at cyanohydrin hydration,

including acetone cyanohydrin hydration. Cyanohydrins are in equilibrium with small amounts of cyanide, and experiments revealed that the Ag–PTA nanoparticles disassemble in the presence of cyanide. The catalyst solution, which is proposed to contain a soluble $Ag(CN)_n^{1-n}$ complex (with n likely equal to 2), remained unpoisoned even in the presence of 10 equiv of cyanide. It is suggested that no cyanide poisoning occurs because the Ag(I) complex is labile. Overall, the Ag–PTA catalyst system (a) is not poisoned by cyanide, (b) catalyzes hydration reactions under mild conditions (in air and at relatively low temperatures), (c) is easily synthesized from cheap starting materials, and (d) can hydrate heteroaromatics in good yields. The recognition of the importance of labile metal cyanide bonding represents an important step forward in catalyst design for improving the catalytic hydration of acetone cyanohydrin.

KEYWORDS: *nitrile hydration, cyanohydrin hydration, nanoparticle catalysis, silver nanoparticles, PTA ligand, water-soluble nanoparticles, cyanide-resistant catalyst*
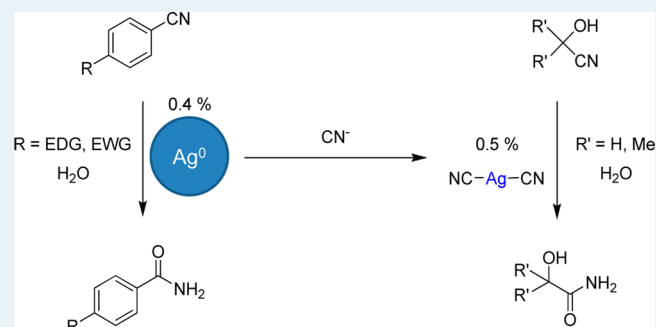
INTRODUCTION

In an industrial setting, the hydration of nitriles to amides is typically performed under extreme conditions.[1] For example, the industrial route for the hydration of acetone cyanohydrin [α-hydroxyisobutyronitrile (ACH), the industrial precursor to methyl methacrylate (MMA)] uses concentrated sulfuric acid (Scheme 1). A major byproduct of this reaction is ammonium hydrogen sulfate (AHS), 2.5 kg of which is formed for every kilogram of MMA produced.[2] This byproduct poses a significant environmental problem and economic disadvantage. To dispose of the 7 million metric tons of AHS produced annually, it is pyrolyzed at 1000 °C to re-form sulfuric acid (Scheme 1).[2,3] This process is energy intensive, and alternate synthetic routes have therefore been sought.[1] A transition metal-catalyzed hydration reaction run under mild conditions would potentially be more economically and environmentally favorable.

Our research group and others have shown that nitriles can be successfully hydrated to their corresponding amides in high yields and under mild conditions with various transition metal catalysts.[1,4,5] Accordingly, we tested many of these same homogeneous catalysts to see if they could be used for the hydration of acetone cyanohydrin. Although the hydration of cyanohydrins would seem to be relatively straightforward, there were complications. Cyanohydrins are in equilibrium with hydrogen cyanide and the corresponding aldehyde or ketone (Scheme 2). When cyanide is present, it can poison a homogeneous catalyst by irreversibly binding to one or more active sites.[6] We previously reported on cyanohydrin hydration with a number of known nitrile hydration catalysts, but only

Scheme 1. Current Chemical Process Used for the Industrial Hydration of Cyanohydrins
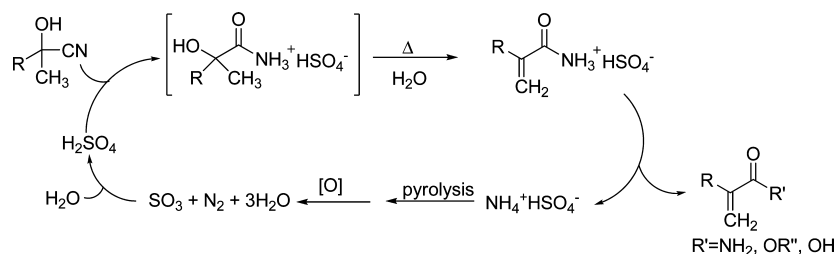
Scheme 2. Equilibrium between a Cyanohydrin and the Corresponding Aldehyde/Ketone and Hydrogen Cyanide[a]
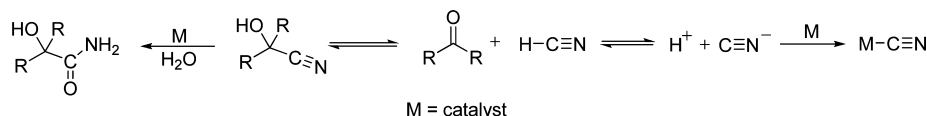
[a]When cyanide is present, it typically binds irreversibly to the metal catalyst, poisoning it.

minimal hydration was observed because of cyanide poisoning.[6,7]

In an effort to find cyanide-resistant catalysts, we turned our attention to nanocatalysts. Nanoparticles are capable of catalyzing a wide variety of reactions,[8] including hydrogenation, dehalogenation, oxidation, and photocatalytic reactions. However, only a handful of investigations have focused on hydration reactions and specifically on nitrile hydration.[9−19] These studies show that nanoparticles have activity comparable to that of homogeneous transition metal catalysts for nitrile hydration. However, no nanoparticle catalysts have been tested for cyanohydrin hydration. In this paper, we report on our investigation of nitrile and cyanohydrin hydration using silver nanoparticles. Because hydration reactions are typically conducted in an aqueous solution, the nanoparticles in this study incorporated a water-soluble stabilizing ligand shell of 1,3,5-triaza-7-phosphaadamantane (PTA), which has been used previously to produce water-soluble nanoparticle catalysts of Pt and Ru.[20]
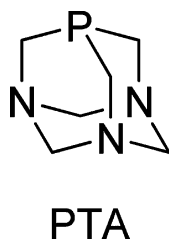

■ RESULTS AND DISCUSSION

Synthesis and Characterization of Ag−PTA Nanoparticles. The Ag−PTA nanoparticles were synthesized by the reduction of silver nitrate with sodium borohydride in cold water (eq 1).

$$AgNO_3 + NaBH_4 \xrightarrow{H_2O, 0\,°C} Ag^0 + 1/2 B_2H_6 + NaNO_3$$

$$(1)$$
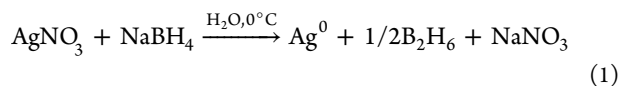
As the AgNO_3 was slowly added to the NaBH_4 over 10 min, the solution in the reaction flask turned from clear to yellow. The yellow color is attributed to the localized surface plasmon resonance (LSPR) of the nanoparticles (λ_{max} = 398 nm) and is evidence that a silver nanoparticle surface is present.[21−23] In the absence of an added ligand, Solomon et al. showed that the

silver nanoparticles are stabilized for a short time by excess borohydride that is adsorbed to the surface of the particles.[24] However, over a period of 30 min, the borohydride decomposes[24] and the nanoparticles precipitate from the solution as bulk metal. To stabilize the particles in this study, PTA was added to the solution immediately after all of the AgNO_3 solution had been added. Experiments showed that a 1.1:1 ratio (PTA:AgNO_3) gave the maximal nanoparticle stability with respect to decomposition or unwanted precipitation.[25] In contrast to the BH_4^−-stabilized particles, the nanoparticles stabilized by PTA remained dispersed in an aqueous solution for several weeks. The PTA-stabilized silver nanoparticles are a slightly darker orange color than the yellow borohydride-stabilized particles. The ultraviolet−visible (UV−vis) spectrum showed a broadening and a decrease in the intensity of the LSPR peak at λ_{max} = 398 nm in the PTA-stabilized particles (Figure 1) compared to that of the
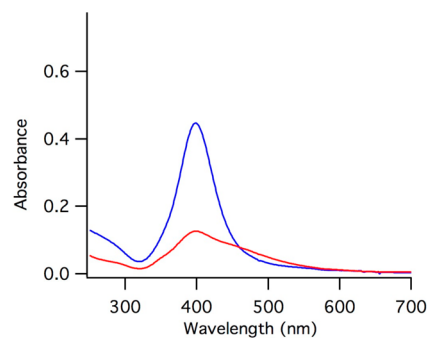
Figure 1. UV−vis spectrum of the localized surface plasmon resonance band of the Ag−PTA nanoparticles before (blue) and after (red) the addition of 1.1 equiv of PTA ligand.

borohydride-stabilized particles. In other studies, the broadening and the decrease in the intensity of the LSPR peak have been attributed to modification of the electronic properties of the nanoparticle surface by the ligand shell.[21,22] A similar explanation is likely applicable here.

The ^{31}P nuclear magnetic resonance (NMR) spectrum of the Ag−PTA nanoparticles showed a peak at −85.6 ppm, assigned to the coordinated PTA ligand. This resonance is shifted downfield and broadened compared to that of uncoordinated PTA, which has a sharp peak at −98.3 ppm (Figure 2). The
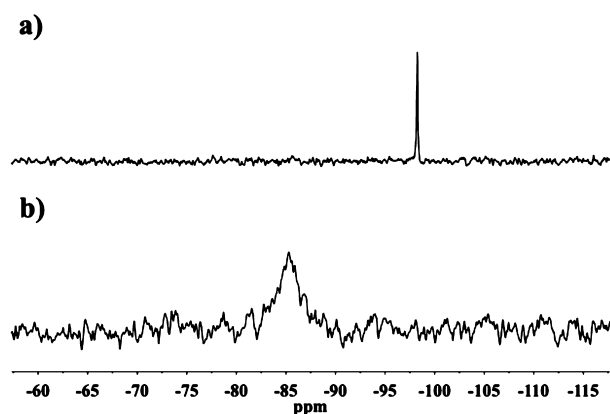
Figure 2. ^{31}P NMR spectrum of (a) the free PTA ligand at −98.3 ppm and (b) the bound PTA ligand on the surface of the Ag−PTA nanoparticles at −85.6 ppm.

broadened peak may be indicative of rapid exchange between between free and bound PTA. However, a number of studies have shown that ligands bonded to nanoparticles typically display broadened and shifted peaks upon coordinating to the nanoparticle.[20,26−28] The broadening and downfield shifts are attributed to the induced shielding of the phosphine ligands when they are bonded to the nanoparticles. Consistent with this latter explanation, it is noted that no resonance for the uncoordinated PTA ligand was observed in the ^{31}P NMR spectrum of the solution containing the nanoparticles, strongly suggesting that all of the PTA is bonded to the surface.

Transmission Electron Microscopy (TEM) Characterization. The size distribution of the Ag−PTA nanoparticles was analyzed by TEM and HRTEM (high-resolution transmission electron microscopy). Prior research showed that $NaBH_4$ reduction of $AgNO_3$ yielded nanoparticles with diameters between 10 and 14 nm.[24] In contrast, TEM images of the Ag−PTA nanoparticles prepared in this study (Figure 3)
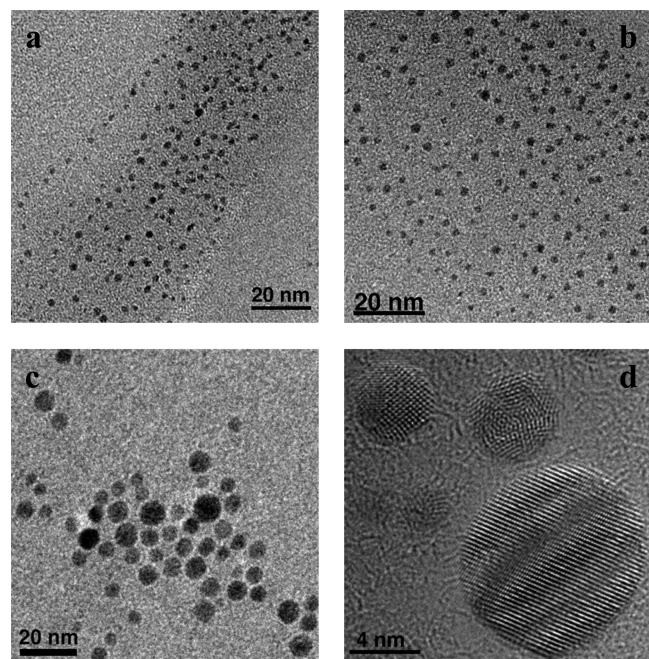
Figure 3. TEM images of (a and b) 2 nm Ag−PTA nanoparticles and (c) 4−10 nm particles and (d) HRTEM image of 4−10 nm particles.

showed an average diameter of 3.5 ± 2 nm (Figure 4). The smaller size of the nanoparticles reported here is attributed to
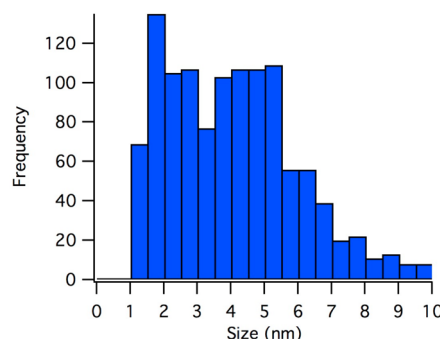
Figure 4. Size distribution histogram of the Ag−PTA nanoparticles (1175 nanoparticles were analyzed).

the PTA ligand. In the preparation described above, PTA was added after the addition of all the $AgNO_3$ to the $NaBH_4$. Prior literature preparations did not use a stabilizing ligand other than excess borohydride. Borohydride does not stabilize the nanoparticles as well as PTA, and in its absence, the nanoparticles precipitate as bulk metal.[29,30] In the case of added PTA, further growth is prevented by coordination of the stronger-binding PTA ligand.
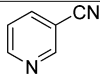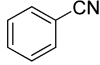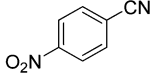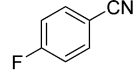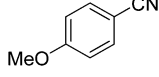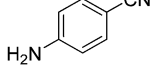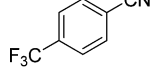
In addition to TEM characterization, the NPs were also analyzed by energy dispersive X-ray spectroscopy (EDS). This technique confirmed that the NPs were composed of Ag (see Figure S1 of the Supporting Information).

Catalysis Studies. A variety of activated and deactivated benzonitriles were hydrated to test the catalytic properties of the Ag−PTA nanoparticles (Table 1). Benzonitrile, a common substrate for testing nitrile hydration,[12,15] was hydrated to benzamide in 90% yield. Initial turnover frequencies (iTOFs) for a range of para-substituted benzonitriles (calculated after reaction for 26 h) followed the trend that hydration becomes faster as the electron-withdrawing ability of the substituent increases, as indicated by the Hammett plot in Figure 5.[6] [The positive slope ($\rho = 1.8$) of the Hammett plot indicates that electron-withdrawing groups facilitate the reaction.] As shown in prior studies,[1,6,31] the correlation between a faster initial turnover frequency and improved substituent electron-withdrawing ability is attributed to the increased electrophilicity of the carbon atom in the nitrile as the electron-withdrawing ability improves. Overall, these results suggest that nucleophilic attack of hydroxide or water is the rate-limiting step, as has been shown previously with homogeneous nitrile hydration catalysts.[1,6] An additional important point to note is that the Ag−PTA nanoparticles are catalytically active for nitrile hydration in air and at relatively mild temperatures (90 °C). In contrast, previously reported Ag nanoparticle catalysts required air-free conditions and temperatures in excess of 150 °C.[12,15,17]

Hydration of several aliphatic nitriles was also examined with the Ag−PTA nanoparticles. Acetonitrile, propionitrile, and methoxyacetonitrile were not hydrated appreciably. It is hypothesized that this lack of activity is due to the increased electron density of the nitrile carbon in these aliphatic systems compared to that of the benzonitriles, making the nucleophilic attack on the nanoparticle-bound substrate less favorable.

Recycling Studies. To test the longevity of the catalyst and to determine if it could be recycled after use, catalyst recycling

Table 1. Selected Nitrile Hydration Results Using Ag−PTA Nanoparticles[a]

entry	nitrile	Hammett sigma value(σ)[32,33]	[nitrile] (M)	catalyst loading mole %	% hydration	rxn time(h)	iTOF (h^{-1})
1	3-cyanopyridine	NA	0.053	0.42	48	282	
2	benzonitrile	0.00	0.049	0.39	90	260	0.86
3	4-nitrobenzonitrile (O_2N)	0.78	0.049	0.38	60	260	21.7
4	4-fluorobenzonitrile (F)	0.06	0.050	0.38	90	337	1.6
5	4-methoxybenzonitrile (MeO)	-0.27	0.050	0.39	44	337	0.46
6	4-aminobenzonitrile (H_2N)	-0.66	0.050	0.39	3.7	337	0.038
7	4-(trifluoromethyl)benzonitrile (F_3C)	0.54	0.050	0.41	90	66	7.18

[a]All reactions were conducted at 90 °C. The catalyst concentration was 0.21 M for all trials except for entry 1, for which it was 0.22 M.
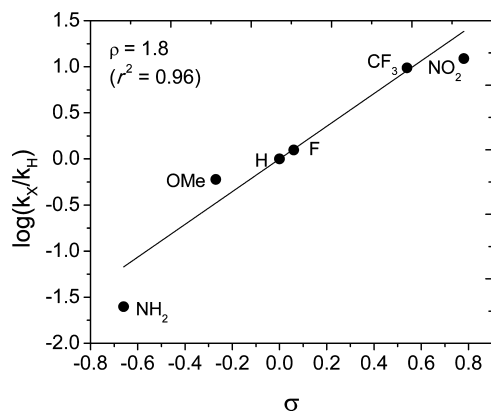

Figure 5. Hammett plot for hydration of para-substituted benzonitriles.

studies were conducted for the hydration of 4-nitrobenzonitrile. After the initial batch of substrate had all reacted, the reaction solution was cooled to 0 °C, causing the 4-nitrobenzamide to crystallize. The product was removed by filtration, and an additional aliquot of 4-nitrobenzonitrile was added to the catalyst solution. The new aliquot of 4-nitrobenzonitrile was also completely converted to 4-nitrobenzamide. The catalyst was reused yet again, without any loss of activity. After recycling, the catalyst was examined by STEM (Figure 6), which showed the nanoparticles were still present and had approximately the same size and shape that they did before they were used in the catalytic reaction.

Cyanohydrin Hydrations. The catalytic activity of the Ag−PTA nanoparticles toward cyanohydrin hydration resulted in several observations. Addition of either acetone cyanohydrin (structure **I** in Chart 1) or glycolonitrile (structure **II** in Chart

1) to the Ag−PTA nanoparticle solution produced an unexpected result: in <30 s, the orange nanoparticle solution became colorless. The UV−vis spectrum of the colorless solution showed the disappearance of the LSPR band at 398 nm, indicating that the nanoparticles had dissolved. Although the Ag−PTA nanoparticles were no longer present, the resulting solution was monitored to see if hydration would occur.

After 504 h, 9.7% of the ACH was hydrated to 2-hydroxyisobutyramide (HIBAM) (Table 2, entry 9). No further conversion was possible because the ACH had decomposed completely to acetone and HCN. For comparison, the best homogeneous catalyst for hydration of ACH, [Ru(η^6-cymene)-Cl$_2$P(NMe$_2$)$_3$], showed a maximum of 15% conversion of ACH to HIBAM in 22 h.[31] (The catalyst was completely poisoned at this point so no further conversion was possible.)

Although all other homogeneous catalysts become inactive because of cyanide poisoning after ACH degradation, the colorless solution generated from the dissolution of the Ag nanoparticles remained active. Addition of more ACH to the solution (after the first 504 h of reaction) resulted in the conversion of the added ACH to HIBAM, indicating that the solution was still catalytically active despite the presence of cyanide. As with the original solution, not all of the additional ACH was hydrated because some of it degraded to acetone and HCN. The solution, however, remained catalytically active because addition of yet a third aliquot of ACH led to more HIBAM. This is a very exciting result because all previous catalysts tested for cyanohydrin hydration have been poisoned after one trial.

Ag−PTA Nanoparticle Dissolution Studies. Studies were next conducted to determine what caused the dissolution of the nanoparticle in the presence of cyanohydrins. As
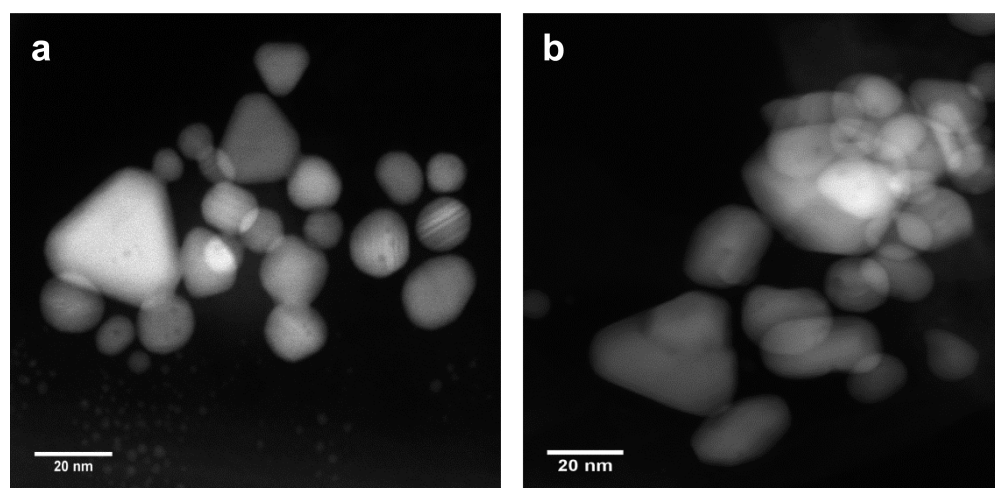
Figure 6. STEM images of PTA-stabilized Ag NPs before (a) and after (b) catalyzing the hydration of benzonitrile. The particles do not undergo drastic changes under catalytic conditions.

Chart 1. Molecular Structures of Acetone Cyanohydrin (I) and Glycolonitrile (II)

mentioned previously, some cyanide is present in these cyanohydrin substrate solutions because of the equilibrium among the cyanohydrin, the aldehyde or ketone, and HCN (Scheme 2).[6] It has been shown in the literature that silver nanoparticles can disassemble to form $Ag(CN)_n$-type complexes in the presence of cyanide and dissolved oxygen.[23,34] It is proposed that this reactivity is also present in the Ag−PTA nanoparticle system. Addition of as little as 0.17 equiv of cyanide to the Ag−PTA nanoparticle solution resulted in the solution becoming colorless almost immediately, accompanied by the disappearance of the LSPR band from the electronic spectrum. Under an inert atmosphere, the nanoparticles persisted for several hours but dissolution eventually occurred. In an inert atmosphere, hydration of ACH proceeded at a rate similar to those of trials conducted in air.

Cyanohydrin Hydration with the Silver Cyanide Solution. Experiments showed that the colorless solution formed by exposure of the Ag−PTA NPs to cyanide was catalytically active. Table 2 (entries 8−13) has five separate ACH hydration trials with varying amounts of cyanide to show the effect of cyanide concentration on the catalyst.

Note that, unusually, the rate of hydration increased as the amount of added cyanide increased. In previous work by our

laboratory, several homogeneous ruthenium nitrile hydration catalysts were found to increase in activity with small amounts (<1 equiv) of added cyanide.[7,31,35] This change was attributed to the electron-withdrawing ability of coordinated cyanide, a feature that facilitates nucleophilic attack of water or hydroxide ion on the coordinated nitrile in a complex with two active sites.[31] However, as the amount of added cyanide increased above 1 equiv, the rate of hydration significantly decreased because cyanide irreversibly bonded to both active sites in the complex. The result of adding cyanide to the nanoparticles did not follow this behavior because excess cyanide did not inhibit the catalytic reactivity. For example, when 0.17 equiv of cyanide was added to the reaction mixture, the rate of hydration increased compared to the case in which no cyanide was added (Table 2, entry 10). However, as further cyanide was added to the reaction mixture (up to 9.3 equiv), the rate of hydration was not affected.

Catalysis with Silver Cyanide Complexes. A control reaction showed that a solution of $AgNO_3$ and KCN hydrated ACH, which suggests that a $Ag(CN)_n^{1-n}$-type complex is capable of hydrating cyanohydrins. Thus, ACH was hydrated to HIBAM in 6.5% yield (Table 3). This result supports the hypothesis that, when the Ag−PTA nanoparticles become oxidized in the presence of oxygen and cyanide, they form a $Ag(CN)_n^{1-n}$-type complex that is capable of hydrating nitriles. Further studies were conducted to determine the specific identity of the active catalyst.

AgCN is known to form insoluble linear coordination polymers in the solid state, and this species was observed as a

Table 2. Hydration of Acetone Cyanohydrin (ACH) Using the Catalytically Active, Colorless Solution Resulting from the Mixing of Ag−PTA Nanoparticles and Cyanohydrins[a]

entry	nitrile	[nitrile] (mM)	[KCN] (mM)	[catalyst] (mM)	catalyst loading (mol %)	equiv of CN^- to Ag atoms	% hydration	reaction time (h)	iTOF (h^{-1})
8	glycolonitrile	68.8	0.0	0.27	0.40	0	4.1	336	
9	ACH	65.3	0.0	0.27	0.41	0	9.7	504	0.078
10	ACH	65.2	0.05	0.27	0.41	0.2	13.8	504	0.087
11	ACH	64.6	0.26	0.27	0.41	1.0	17.1	504	0.09
12	ACH	61.8	1.26	0.25	0.41	5.0	14.5	843	0.1
13	ACH	61.5	2.26	0.24	0.39	9.3	17.1	843	0.093

[a]All reactions were conducted at 90 °C.

Table 3. Hydration Reactions with Silver Cyanide Complexes[a]

entry	nitrile	catalyst	[nitrile] (M)	[catalyst] (mM)	catalyst loading (mol %)	% hydration	reaction time (h)	iTOF (h^{-1})
14	ACH	$AgNO_3$(aq) and KCN(aq)	0.063	2.70	4.3	6.5	499	0.01
15	ACH	$KAgCN_2$(aq)	0.049	0.25	0.52	6.5	216	0.14
16	benzonitrile	$KAgCN_2$(aq)	0.048	0.25	0.52	50	216	0.7
17	ACH	$KAgCN_2$(aq) and PTA(aq)	0.048	0.25	0.52	6.0	216	0.13
18	ACH	$KAgCN_2$(aq) and KCN(aq)	0.048	0.25	0.52	6.0	216	0.13

[a]All reactions were conducted at 90 °C.

Table 4. Control Reactions for the Hydration of *p*-Nitrobenzonitrile

entry	catalyst	[nitrile] (M)	[catalyst] (mM)	catalyst loading (mol %)	reaction temperature (°C)	iTOF (h^{-1})	% hydration	reaction time (h)
19	Ag–PTA nanoparticles	0.052	0.21	0.40	90	23.5	48	22
20	$AgNO_3$(aq)	0.057	0.24	0.42	90	1.4	11	19
21	$AgNO_3$(aq) and 4PTA(aq)	0.057	0.24	0.42	90	1.8	14	19

precipitate in the solution of $AgNO_3$ and KCN.[36−38] Therefore, this polymer is unlikely to be the active catalyst. It is more likely that a water-soluble, anionic complex such as $[Ag(CN)_2]^-$ catalyzes the hydration reaction. To test this hypothesis, we tested the commercially available salt $K[Ag(CN)_2]$ as a catalyst for nitrile and cyanohydrin hydration. Benzonitrile and ACH were tested as substrates, and hydration of both species was observed (Table 3, entries 15 and 16). Addition of PTA to the catalyst solution did not affect the rate of hydration (Table 3, entry 17). Furthermore, the presence of additional CN^- did not significantly change the rate (Table 3, entry 18). These experiments allow for two conclusions. First, the species formed in the nanoparticle solutions is likely a complex of the form $Ag(CN)_n^{n-1}$. The $Ag(CN)_2^-$ complex is suggested, but similar complexes are possible, as well. Second, the increase in the hydration rate in the presence of larger quantities of cyanide in the initial trials using the nanoparticle solution as the catalyst was not due to the cyanide itself. Rather, as more cyanide was added, more of the active catalyst species [probably $Ag(CN)_2^-$] formed. The increased concentration of the catalyst caused the hydration reaction to proceed at a faster rate.

The resistance of the $Ag(CN)_2^-$ complex to cyanide poisoning likely results from the lability of bonds to the d^{10} Ag(I) metal center. Thus, cyanide reversibly binds to the Ag center. Binding sites therefore remain available for the substrate. The greater activity of the anionic $Ag(CN)_2^-$ complex compared to that of Ag(I) alone (i.e., in the absence of cyanide) is attributed to the electron-withdrawing ability of the cyanide.[1]

Control Reactions. Control experiments showed that aqueous Ag^+ (from $AgNO_3$) is a catalyst for nitrile hydration; however, the rate of hydration is slow compared to that of the Ag–PTA nanoparticles. (Compare entries 19 and 20 in Table 4.)

Solutions of $AgNO_3$ and PTA form coordination polymers in which the PTA ligands bind silver through both P and N sites.[39] This polymer was synthesized, and it had a catalytic activity similar to that of aqueous $AgNO_3$.

The pH of the aqueous Ag–PTA NP solution was 8. To ensure that the reaction was not base-catalyzed, hydration trials with benzonitrile and ACH were conducted at this pH with no added catalyst or ligand. No reactivity was observed over 72 h.

CONCLUSIONS

This study prepared water-soluble Ag nanoparticles with a PTA ligand shell, in which PTA is a water-soluble phosphine ligand. The Ag–PTA nanoparticles are nitrile hydration catalysts, as demonstrated by their ability to hydrate a variety of aromatic nitriles with various steric and electronic properties at rates comparable to those of some common homogeneous catalysts.[1] The Ag–PTA nanoparticle catalysts have three particularly noteworthy properties. (1) They catalyze hydration reactions under mild conditions (i.e., in air at relatively low temperatures). (2) They are easily synthesized from cheap starting materials. (3) They can hydrate heteroaromatics in good yields.

Solutions of the Ag–PTA NPs are also catalysts for the hydration of cyanohydrins. Remarkably, the catalyst solution could be recycled without any loss of activity or evidence of cyanide poisoning. Closer examination, however, showed that Ag NPs were not the catalyst but rather a Ag(I)−cyanide complex, likely $Ag(CN)_2^-$, was the active catalyst. This is a notable result because cyanide poisoning in cyanohydrin hydration reactions has been an intractable problem that has plagued the homogeneous catalytic hydration of cyanohydrins. In short, all homogeneous catalysts studied to date are poisoned by cyanide. The results presented in this paper suggest a strategy for overcoming the poisoning problem. Specifically, the insensitivity of the $Ag(CN)_2^-$ catalyst to cyanide poisoning is attributed to the lability of the Ag(I) metal center, which suggests it will be worthwhile to examine the catalytic hydration abilities of other complexes with labile electronic configurations. Although low TOFs are still a problem, a judicious choice of ligands in these complexes may help to alleviate the slow rates. Alternatively, strategies that stabilize ACH and prevent it from forming HCN, namely a strongly acidic medium, may prove viable. Both strategies are currently being investigated in our laboratory.

EXPERIMENTAL SECTION

Instrumentation and Procedures. Nuclear magnetic resonance spectra were recorded on a Varian Unity/Inova 500 MHz (^{1}H, 500.10 MHz; ^{31}P, 202.45 MHz; ^{13}C, 151 MHz) spectrometer or on a Bruker Biospin 600 MHz (^{1}H, 600.02 MHz; ^{31}P, 242.83 MHz) spectrometer. The ^{1}H chemical shifts were referenced to the solvent peak or TMS (0.00 ppm), and the ^{31}P chemical shifts were referenced to H_3PO_4 (0.00 ppm). The solvent used for all NMR trials was D_2O. UV−vis spectra

were recorded on an HP 8453 spectrometer using 1 cm quartz cuvettes. All hydration reaction samples were prepared in 1 dram screwcap vials fitted with septum caps. (HR)TEM images were acquired with a FEI Titan 80−300 kV transmission electron microscope equipped with a spherical aberration (C_s) image corrector, an EDAX energy dispersive spectrometer, and a Tridiem 863 Gatan imaging filter and electron energy loss spectrometer. All images were acquired at 300 kV. PTA was synthesized via literature methods.[40]

Preparation of 1,3,5-Triaza-7-phosphaadamantane (PTA)-Stabilized Silver Nanoparticles. A preparation from the group of S. D. Solomon for uncapped silver nanoparticle synthesis was modified.[17] $NaBH_4$ (0.0082 g, 0.217 mmol) was dissolved in 90 mL of water and the mixture placed in an ice bath while being magnetically stirred. $AgNO_3$ (0.0059 g, 0.035 mmol) was dissolved in 30 mL of water and the mixture added over 10 min to the cool $NaBH_4$ solution. The solution turned yellow, characteristic of silver nanoparticles. After the particles had been formed, PTA (0.0061 g, 0.039 mmol) dissolved in 10 mL of water was added to the solution as a stabilizer. Samples were prepared for TEM on a lacey carbon grid with an ultrathin (3 nm) carbon support film supported by copper mesh. A dilute nanoparticle solution was dropped on the grid and allowed to evaporate.

General Procedure for the Hydration of Benzonitrile with PTA-Stabilized Ag NPs. Benzonitrile (10 μL, 0.09 mmol) was added to 1000 μL of a 0.22 mM Ag NP solution and heated to 90 °C while being stirred. Aliquots (100 μL) were removed periodically using a gastight syringe and combined in an NMR tube with 500 μL of a 2.28 mM NMe_4PF_6 solution in D_2O as an internal standard. The progress of the reaction was monitored by observing the disappearance of the benzonitrile resonances at 7.70 ppm (d, J = 7.48 Hz), 7.65 ppm (t, J = 7.85 Hz), and 7.49 ppm (t, J = 7.87 Hz) and the appearance of the amide resonances at 7.78 ppm (m) and 7.15 ppm (t, J = 7.97 Hz) in the ^{1}H NMR spectrum of the mixture.

General Procedure for the Hydration of Para-Substituted Benzonitriles with PTA-Stabilized Ag NPs. The nitrile was dissolved in 2 mL of acetone and the mixture added to the 0.22 mM catalyst solution to achieve a concentration of approximately 50 mM. This solution was heated to 90 °C while being stirred. Aliquots (100 μL) were removed periodically using a gastight syringe and combined in an NMR tube with 500 μL of a 2.28 mM solution of NMe_4PF_6 in D_2O. Specific details for individual nitriles are as follows.

p-Fluorobenzonitrile. The progress of the reaction was monitored by observing the disappearance of the aromatic p-fluorobenzonitrile resonances at 7.78 ppm (m) and 7.24 ppm (t, J = 8.8 Hz) and the appearance of the amide resonances at 7.79 ppm (m) and 7.17 ppm (t, J = 9.1 Hz) in the ^{1}H NMR spectrum.

p-Nitrobenzonitrile. The progress of the reaction was monitored by observing the disappearance of the aromatic p-nitrobenzonitrile resonances at 8.32 ppm (d, J = 8.5 Hz) and 7.96 ppm (d, J = 8.7 Hz) and the appearance of the amide resonances at 8.27 (d, J = 8.6 Hz) and 7.92 ppm (d, J = 8.9 Hz) in the ^{1}H NMR spectrum.

p-Methoxybenzonitrile. The progress of the reaction was monitored by observing the disappearance of the aromatic p-methoxybenzonitrile resonances at 7.66 ppm (d, J = 8.7 Hz) and 7.02 ppm (d, J = 8.8 Hz) and the appearance of the amide

resonances at 7.74 ppm (d, J = 8.6 Hz) and 7.01 ppm (d, J = 8.7 Hz) in the ^{1}H NMR spectrum.

p-Aminobenzonitrile. The progress of the reaction was monitored by observing the disappearance of the aromatic p-aminobenzonitrile resonance at 7.43 ppm (d, J = 8.5 Hz) and the appearance of the amide resonance at 7.57 ppm (d, J = 8.4 Hz) in the ^{1}H NMR spectrum.

p-Trifluoromethylbenzonitrile. The progress of the reaction was monitored by observing the disappearance of the aromatic p-trifluoromethylbenzonitrile resonances at 7.89 ppm (d, J = 8.4 Hz) and 7.82 ppm (d, J = 8.0 Hz) and the appearance of the amide resonances at 7.87 ppm (d, J = 8.3 Hz) and 7.77 ppm (d, J = 8.1 Hz) in the ^{1}H NMR spectrum.

Hydration of Nicotinonitrile with PTA-Stabilized Ag NPs. Nicotinonitrile (0.0493 g, 0.474 mmol) was added to 1 mL of acetone. This solution (125 μL) was added to 1000 μL of a 0.22 mM Ag NP solution. The mixture was heated to 90 °C while being stirred. Aliquots (100 μL) were removed periodically using a gastight syringe and combined in an NMR tube with 450 μL of D_2O and 50 μL of a 10.86 mM NMe_4PF_6 internal standard solution in D_2O. The progress of the reaction was monitored by observing the disappearance of the nicotinonitrile resonance at 8.81 ppm and the appearance of the amide resonance at 8.73 ppm.

Hydration of ACH with PTA-Stabilized Ag NPs. ACH (10 μL, 0.109 mmol) was added to 1750 μL of a 0.22 mM Ag NP solution. This solution was heated to 90 °C while being stirred. After 264 h, an additional 0.082 mmol of ACH (7.5 μL) was added to the reaction vessel. Aliquots (100 μL) were removed periodically using a gastight syringe and combined in an NMR tube with 450 μL of D_2O and 50 μL of a 10.86 mM NMe_4PF_6 internal standard solution in D_2O. The progress of the reaction was monitored by observing the disappearance of the methyl resonance of acetone cyanohydrin at 1.57 ppm [s, 6H, $HO(CH_3)_2CCN$] and the appearance of the amide resonance at 1.34 ppm [s, $HO(CH_3)_2CC(O)NH_2$].

Hydration of p-Nitrobenzonitrile with $AgNO_3$. $AgNO_3$ (0.006 g, 0.03 mmol) was dissolved in 10 mL of water. Nitrobenzonitrile (0.0408 g, 0.275 mmol) was dissolved in 1 mL of acetone-d_6. The p-nitrobenzonitrile solution (400 μL) and the $AgNO_3$ solution (130 μL) were added to 1400 μL of water in a 1 dram screwcap vial capped with a septum. This mixture was heated to 90 °C while being stirred. Aliquots (100 μL) were removed periodically using a gastight syringe and combined in an NMR tube with 450 μL of D_2O and 50 μL of a 10.86 mM NMe_4PF_6 internal standard solution in D_2O. The progress of the reaction was monitored by observing the disappearance of the p-nitrobenzonitrile resonance at 8.32 ppm (d, J = 8.5 Hz) and the appearance of the amide resonance at 8.27 ppm (d, J = 8.6 Hz) in the ^{1}H NMR spectrum.

Hydration of p-Nitrobenzonitrile with $AgNO_3$ and 4 equiv of PTA. Nitrobenzonitrile (0.0408 g, 0.275 mmol) was dissolved in 1 mL of acetone-d_6. $AgNO_3$ (0.006 g, 0.0353 mmol) was dissolved in 10 mL of water. PTA (0.0088 g, 0.0566 mmol) was added to 4 mL of the $AgNO_3$ solution. The p-nitrobenzonitrile solution (400 μL) and the $AgNO_3$/PTA solution (130 μL) were added to 1400 μL of water. This mixture was heated to 90 °C while being stirred in a 1 dram screwcap vial capped with a septum. Aliquots (100 μL) were removed periodically using a gastight syringe and combined in an NMR tube with 450 μL of D_2O and 50 μL of a 10.86 mM NMe_4PF_6 internal standard solution in D_2O. The progress of the reaction was monitored by observing the disappearance of

the *p*-nitrobenzonitrile resonance at 8.32 ppm (d, *J* = 8.5 Hz) and the appearance of the amide resonance at 8.27 (d, *J* = 8.6 Hz) in the ^{1}H NMR spectrum.

Hydration of ACH with AgNO₃ and KCN. ACH (10 μL, 0.109 mmol) was added to a solution containing 100 μL of AgNO₃ (58.87 mM) and varying amounts of KCN (24.5 mM) that had been diluted to 1610 μL. This mixture was heated to 90 °C while being stirred in a 1 dram screwcap vial with a septum cap. Aliquots (100 μL) were removed periodically using a gastight syringe and combined in an NMR tube with 500 μL of a 10.86 mM NMe₄PF₆ solution in D₂O. The progress of the reaction was monitored by observing the disappearance of the methyl resonance of acetone cyanohydrin at 1.57 ppm [s, 6H, HO(CH₃)₂CCN] and the appearance of the amide resonance at 1.34 ppm [s, HO(CH₃)₂CC(O)NH₂].

General Procedure for the Hydration of ACH with KAg(CN)₂. ACH (10 μL, 0.109 mmol) was added to 1000 μL of a 5.03 mM solution of KAg(CN)₂ in water. In some cases, a solution of PTA (100 μL of a 50 mM solution in H₂O) was added to the catalyst solution. This solution was heated to 90 °C while being stirred in a 1 dram screwcap vial capped with a septum. Aliquots (100 μL) were removed periodically using a gastight syringe and combined in an NMR tube with 500 μL of a 10.86 mM NMe₄PF₆ internal standard solution in D₂O. The progress of the reaction was monitored by observing the disappearance of the methyl resonance of acetone cyanohydrin at 1.57 ppm [s, 6H, HO(CH₃)₂CCN] and the appearance of the amide resonance at 1.34 ppm [s, HO(CH₃)₂CC(O)NH₂].

Hydration of Benzonitrile with KAg(CN)₂. Benzonitrile (10 μL, 0.0969 mmol) was added to 1000 μL of a 5.03 mM solution of KAg(CN)₂ in water. This mixture was heated to 90 °C while being stirred in a 1 dram screwcap vial capped with a septum. Aliquots (100 μL) were removed periodically using a gastight syringe and combined in an NMR tube with 500 μL of a 10.86 mM NMe₄PF₆ internal standard solution in D₂O. The progress of the reaction was monitored by observing the disappearance of the benzonitrile resonance at 7.49 ppm (t, *J* = 7.87 Hz) and the appearance of the amide resonance at 7.15 ppm (t, *J* = 7.97 Hz) in the ^{1}H NMR spectrum of the mixture.

pH Studies. The pH of the aqueous Ag−PTA NP solution was 8. Hydration trials at this pH (with no added catalyst or ligand) resulted in no reactivity over 72 h.

■ ASSOCIATED CONTENT

Ⓢ Supporting Information

Experimental procedure for the air-free hydration of ACH and EDX spectrum of the Ag−PTA nanoparticles. This material is available free of charge via the Internet at http://pubs.acs.org.

■ AUTHOR INFORMATION

Corresponding Author
*E-mail: dtyler@uoregon.edu.

Author Contributions
T.J.S. and E.L.D. contributed equally to this work.

Notes
The authors declare no competing financial interest.

■ ACKNOWLEDGMENTS

■ REFERENCES

(1) Ahmed, T. J.; Knapp, S. M. M.; Tyler, D. R. *Coord. Chem. Rev.* **2011**, *255*, 949−974.
(2) Green, M. M.; Witcoff, H. A. *Organic Chemistry Principles and Industrial Practice*; Wiley-VCH: Weinheim, Germany, 2003.
(3) Bizzari, S. *Chemical Economics Handbook*; SRI Consulting: Menlo Park, CA, 2010.
(4) García-Álvarez, R.; Crochet, P.; Cadierno, V. *Green Chem.* **2013**, *15*, 46.
(5) Kukushkin, V. Y.; Pombeiro, A. J. L. *Inorg. Chim. Acta* **2005**, *358*, 1−21.
(6) Ahmed, T. J.; Fox, B. R.; Knapp, S. M. M.; Yelle, R. B.; Juliette, J. J.; Tyler, D. R. *Inorg. Chem.* **2009**, *48*, 7828−7837.
(7) Knapp, S. M. M.; Sherbow, T. J.; Juliette, J. J.; Tyler, D. R. *Organometallics* **2012**, *31*, 2941−2944.
(8) Yan, N.; Xiao, C.; Kou, Y. *Coord. Chem. Rev.* **2010**, *254*, 1179−1218.
(9) Shimizu, K.; Kubo, T.; Satsuma, A.; Kamachi, T.; Yoshizawa, K. *ACS Catal.* **2012**, *2*, 2467−2474.
(10) Subramanian, T.; Pitchumani, K. *Catal. Commun.* **2012**, *29*, 109−113.
(11) Ishizuka, A.; Nakazaki, Y.; Oshiki, T. *Chem. Lett.* **2009**, *38*, 360−361.
(12) Kim, A. Y.; Bae, H. S.; Park, S.; Park, S.; Park, K. H. *Catal. Lett.* **2011**, *141*, 685−690.
(13) Hirano, T.; Uehara, K.; Kamata, K.; Mizuno, N. *J. Am. Chem. Soc.* **2012**, *134*, 6425−6433.
(14) Liu, Y.-M.; He, L.; Wang, M.-M.; Cao, Y.; He, H.-Y.; Fan, K.-N. *ChemSusChem* **2012**, *5*, 1392−1396.
(15) Mitsudome, T.; Mikami, Y.; Mori, H.; Arita, S.; Mizugaki, T.; Jitsukawa, K.; Kaneda, K. *Chem. Commun.* **2009**, 3258−3260.
(16) Baig, R. B. N.; Varma, R. S. *Chem. Commun.* **2012**, *48*, 6220−6222.
(17) Shimizu, K.; Imaiida, N.; Sawabe, K.; Satsuma, A. *Appl. Catal., A* **2012**, *421−422*, 114−120.
(18) Polshettiwar, V.; Varma, R. S. *Chem.—Eur. J.* **2009**, *15*, 1582−1586.
(19) Woo, H.; Lee, K.; Park, S.; Park, K. H. *Molecules* **2014**, *19*, 699−712.
(20) Debouttière, P.-J.; Coppel, Y.; Denicourt-Nowicki, A.; Roucoux, A.; Chaudret, B.; Philippot, K. *Eur. J. Inorg. Chem.* **2012**, *2012*, 1229−1236.
(21) Hendrich, C.; Bosbach, J.; Stietz, F.; Hubenthal, F.; Vartanyan, T.; Träger, F. *Appl. Phys. B: Lasers Opt.* **2003**, *76*, 869−875.
(22) Lismont, M.; Dreesen, L. *Mater. Sci. Eng., C* **2012**, *32*, 1437−1442.
(23) Hajizadeh, S.; Farhadi, K.; Forough, M.; Sabzi, R. E. *Anal. Methods* **2011**, *3*, 2599−2603.
(24) Mulfinger, L.; Solomon, S. D.; Bahadory, M.; Jeyarajasingam, A. V.; Rutkowsky, S. A.; Boritz, C. *J. Chem. Educ.* **2007**, *84*, 322.
(25) Solutions in which a <1.1:1 PTA:AgNO₃ molar ratio was added yielded unstable nanoparticles that crashed out of solution after ~30 min. Solutions in which a >2:1 PTA:AgNO₃ molar ratio was added yielded unstable particles that caused the nanoparticle solution to turn colorless.
(26) Deboutière, P.-J.; Martinez, V.; Philippot, K.; Chaudret, B. *Dalton Trans.* **2009**, 10172−10174.
(27) Son, S. U.; Jang, Y.; Yoon, K. Y.; Kang, E.; Hyeon, T. *Nano Lett.* **2004**, *4*, 1147−1151.
(28) Wu, L.; Li, Z.-W.; Zhang, F.; He, Y.-M.; Fan, Q.-H. *Adv. Synth. Catal.* **2008**, *350*, 846−862.
(29) Madras, G.; McCoy, B. J. *J. Chem. Phys.* **2002**, *117*, 8042−8049.
(30) Marquse, J. A.; Ross, J. *J. Chem. Phys.* **1983**, *79*, 373−378.
(31) Knapp, S. M. M.; Sherbow, T. J.; Yelle, R. B.; Zakharov, L. N.; Juliette, J. J.; Tyler, D. R. *Organometallics* **2013**, *32*, 824−834.
(32) Hammett, L. P. *J. Am. Chem. Soc.* **1937**, *59*, 96−103.
(33) Hansch, C.; Leo, A.; Taft, R. W. *Chem. Rev.* **1991**, *91*, 165−195.
(34) Ghosh, S. K.; Kundu, S.; Pal, T. *Bull. Mater. Sci.* **2002**, *25*, 581−582.

(35) Knapp, S. M. M.; Sherbow, T. J.; Yelle, R. B.; Juliette, J. J.; Tyler, D. R. *Organometallics* **2013**, *32*, 3744−3752.

(36) Bayse, C. A.; Ming, J. L.; Miller, K. M.; McCollough, S. M.; Pike, R. D. *Inorg. Chim. Acta* **2011**, *375*, 47−52.

(37) Bryce, D. L.; Wasylishen, R. E. *Inorg. Chem.* **2002**, *41*, 4131−4138.

(38) Bowmaker, G. A.; Kennedy, B. J.; Reid, J. C. *Inorg. Chem.* **1998**, *37*, 3968−3974.

(39) Mohr, F.; Falvello, L. R.; Laguna, M. *Eur. J. Inorg. Chem.* **2006**, *2006*, 3152−3154.

(40) Daigle, D. J. *Inorg. Synth.* **1998**, *32*, 40−45.